The Asymmetric Seismic Moment Tensor in Micropolar Media

by Rafael Abreu,[*] Stephanie Durand, and Christine Thomas

Abstract Coseismic block rotations are observed in the vicinity of seismogenic faults and have an effect on the moment tensor. This can be accounted for using the linear micropolar theory, which allows the existence of an independent rotation or spin θ different from the continuum rotation $1/2$ curl u. In this study, we show that the use of micropolar theory yields asymmetric seismic moment tensors that allow a momentum exchange between the rotational microstructure in the source region and the rest of the Earth and thus explicitly accounts for microstructural rupture processes, which naturally engages a macroscopic displacement response. This work provides a theoretical framework for the development of future dynamic source inversions using micropolar theory.

Introduction

Being able to describe seismic source mechanisms is a key point in seismology to better understand the origin of earthquakes and in particular to relate them to the geological context. The effect and influence of microscale processes in the description of earthquakes' sources is an active area of research (see, e.g., Miguel *et al.*, 2006; Renard *et al.*, 2013; Raziperchikolaee *et al.*, 2014a,b; Pluymakers *et al.*, 2017; Tarasov, 2017). These effects are commonly avoided in numerical simulations due to significant complications arising in the mathematical description and numerical formulation of the problem (Ampuero *et al.*, 2002; de la Puente *et al.*, 2009; Pelties *et al.*, 2012). However, they can be studied through the application of microcontinuum field theories (Eringen, 1999).

The theories of microcontinuum media denote generalized elastic theories with enriched kinematics, in which each particle inside the elastic medium has additional degrees of freedom of deformation. They are divided into three main categories: micropolar (Cosserat), microstretch, and micromorphic media. The simplest case is the first one, the theory of micropolar media, also called the Cosserat's theory (Cosserat and Cosserat, 1909), which includes additional rotational degrees of freedom at each spatial location (Eringen and Kafadar, 1976; Nowacki, 1986; Neff and Jeong, 2009; Jeong and Neff, 2010). It can thus account for the existence of an independent rotation of each particle of the elastic medium, called spin θ, different from the continuum rotation $1/2$ curl u.

The term "micro" in microcontinuum field theories is, however, unfortunate and misleading because it refers to the scale of the particles that are rotating, with respect to the scale of the considered elastic media, whichever is their

actual size, microscopic, mesoscopic, or macroscopic. The scale term "micro" thus depends on the problem it is applied to. For instance, microcontinuum field theories can be used for describing the deformation at tectonic scales. Then "micro" refers to the size of the approximately 1–10-km rotating blocks, which can be considered as micro with respect to the scale of tectonic plates (Unruh *et al.*, 1996). The theories can also be applied for describing the deformation at the scale of minerals; the microscale then refers to the size of individual molecules that is micro with respect to the arrangement of crystals (Abreu, Thomas, *et al.*, 2017). The application of microcontinuum field theories is thus wide and aims to connect different scales varying from atomistic- to large-scale tectonics.

In general, the connection between microscale and macroscale phenomena is achieved using homogenization or averaging techniques (Capdeville *et al.*, 2013; Fichtner *et al.*, 2013; Choy, 2016). The goal of these averaging techniques is to find what is called the best effective homogenized model that is able to reproduce the macroscopic mechanical behavior of some material while omitting the microscopic scale complexities. This is a powerful tool for simplifying some physical phenomena in complex media such as seismic-wave propagation in layered or anisotropic media (Capdeville *et al.*, 2013). However, these techniques imply that the exact information on the microscale is lost, sometimes even introducing artifacts (Wang *et al.*, 2013). This can be avoided using enriched continuum theories that are able to describe the desired properties of the considered materials at the large scale, explicitly including microstructural effects (d'Agostino *et al.*, 2018).

The first work that introduced microcontinuum field theories in source seismology was, to our knowledge, by Teisseyre (1973). Since then, micropolar theory has been repeatedly used for the kinematic description of earthquake

*Also at Instituto Andaluz de Geofísica, Universidad de Granada, Campus de Cartuja s/n, E-18071 Granada, Spain.

seismic sources (Twiss *et al.*, 1991, 1993; Unruh *et al.*, 1996, 2003; Wojtal, 2001; Teisseyre *et al.*, 2006; Lewis *et al.*, 2008; Schemmann *et al.*, 2008; Twiss, 2009; Gade and Raghukanth, 2016) and modeling localization phenomena (Schijve, 1966; Sharbati and Naghdabadi, 2006).

In the case of the kinematic description of earthquake seismic sources, this theory includes the kinematic effects of block rotations and the authors conclude that they can better describe the deformation with the use of micropolar theory (Twiss *et al.*, 1991; Wojtal, 2001; Unruh *et al.*, 2003; Lewis *et al.*, 2008; Schemmann *et al.*, 2008). Specifically, the solution to the micropolar inverse problem relates the seismic P and T axes to the orientation of the principal axes of the global strain-rate tensor (the term global strain-rate tensor refers to the strain-rate tensor at the large tectonic scale; Unruh *et al.*, 1996). In adopting this deformation interpretation, the authors argue that the measurements, by which the P and T axes are defined, are directly related to the displacement on the fault. It means that (1) the seismic P and T axes define the local principal strain-rate axes, not the local principal stress axes; (2) the slip directions on the shear planes are the directions of the maximum resolved rate of shear of the global deformation rather than the direction of the maximum resolved shear stress; and (3) the inversion provides the orientations and relative magnitudes of the principal global strain rates, not the principal global stresses. This difference in approach has allowed Twiss *et al.* (1991) to derive the effects of rigid block rotations on the slip directions and Twiss *et al.* (1993) to derive the effects on the asymmetric part of the generalized micropolar seismic moment tensor. Micropolar inversion is unique in accounting for possible block rotations, and Unruh *et al.* (1996, 2003) and Lewis *et al.* (2008) argue that the results of the inversion are better interpreted as the deformation rather than the stress. The results presented by Unruh *et al.* (1996) support the hypothesis that coseismic block rotations have an observable effect on focal mechanism solutions. The use of the micropolar model for inverting the aftershock focal mechanisms thus leads to a more complete description of the deformation within seismogenic shear zones.

In the case of the modeling of localization phenomena, the major advantage of the Cosserat theory with respect to the classical linear theory (Schijve, 1966; Sharbati and Naghdabadi, 2006) is a better description of the brittle deformation. Indeed, distributed brittle deformation in the Earth's crust is characterized by granular substructure for which the grains are effectively rigid blocks, and the fault planes are the boundaries of the blocks (Luyendyk *et al.*, 1980; Wells and Heller, 1988; Kissel and Laj, 2012). A distributed brittle deformation can be described with the classical linear elastic theory but only if the discontinuous slip on fault planes is assumed to be averaged over a local volume of the material, that is, if the discontinuous slip is large relative to the distance between the discontinuities. Under this condition, the linear elastic theory gives rise to a symmetric moment tensor, although several geodesy studies (see, e.g.,

Molnar and Qidong, 1984; Peltzer *et al.*, 1999) suggested that it should be asymmetric because an asymmetric deformation and velocity gradient field has been observed in major shear zones. An asymmetric moment tensor allows a momentum exchange between the rotational microstructure in the source region and the rest of the Earth. The momentum exchange is produced by redistribution of mass during the seismic event. It has been previously shown that this momentum exchange corresponds to nonlinear terms in the theory of wave propagation (Takei and Kumazawa, 1994). The physical justification for this momentum exchange is the presence of mass advection in the rupture process or events occurring on the Earth's surface involving a detached mass such as landslides or volcanic earthquakes related to magmatic activity. The linear elastic theory fails to account for these effects.

Here, we present the dynamic description of the seismic source using the linear micropolar theory. We first give a brief motivation for the use of micropolar theory in seismology. We then recall the formal description of the equations of motion in micropolar media, explain concepts of strain and stress glut source (Backus and Mulcahy, 1976a,b) and strain and stress Green's tensors, and finish with the illustration of the slip on an ideal fault described by the linear micropolar model.

Motivation for the Use of Micropolar Theory Using Rotational Sensor Records

The introduction of a new theory should be motivated by observations that cannot be explained with theories currently in use. With this, the main motivation of micropolar theory in seismology comes from the insufficiencies of the conventional linear elasticity to coherently include rotational motions (Nagahama and Teisseyre, 2000; Teisseyre *et al.*, 2006, 2008; Teisseyre, 2008, 2011). In conventional elasticity, rotational motions $\boldsymbol{\omega}$ are computed using the curl operator (e.g., Bernauer *et al.*, 2009; Lee *et al.*, 2009; van Driel *et al.*, 2012; Nader *et al.*, 2015) as follows:
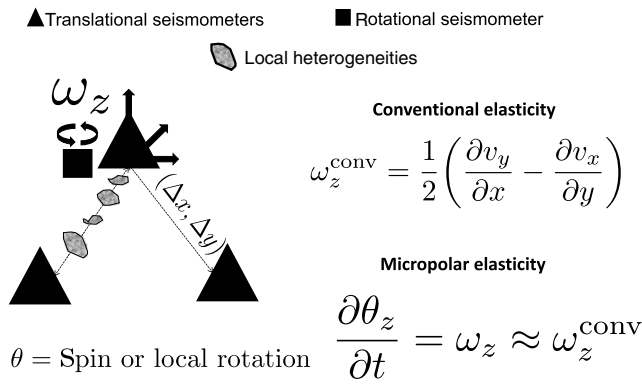
$$\begin{pmatrix} \omega_x \\ \omega_y \\ \omega_z \end{pmatrix} = \frac{1}{2} \operatorname{curl} v = \frac{1}{2} \begin{pmatrix} \partial_y v_z - \partial_z v_y \\ \partial_z v_x - \partial_x v_z \\ \partial_x v_y - \partial_y v_x \end{pmatrix}, \qquad (1)$$

in which v is the velocity field and $\boldsymbol{\omega}$ is the vertical rotation rate. Equation (1) shows that information on the gradient of the displacement in the horizontal planes ($\partial_x v_y - \partial_y v_x$) are needed to compute ω_z, for instance.

In practice, the vertical coordinate of the rotation rate ω_z can be approximated using the velocity records provided by translational seismometers as follows:

$$\omega_z \approx \frac{1}{2} \left(\frac{\Delta v_y}{\Delta x} - \frac{\Delta v_x}{\Delta y} \right), \qquad (2)$$

in which Δ is the difference operator.

$$\omega_z$$

$$\theta = \text{Spin or local rotation}$$

Conventional elasticity

$$\omega_z^{\text{conv}} = \frac{1}{2}\left(\frac{\partial v_y}{\partial x} - \frac{\partial v_x}{\partial y}\right)$$

Micropolar elasticity

$$\frac{\partial \theta_z}{\partial t} = \omega_z \approx \omega_z^{\text{conv}}$$

Figure 1. Rotational seismology using conventional and micropolar elasticity.

In conventional elasticity, the partial derivatives in equation (1) have thus been replaced by differential approximations in equation (2) (Spudich *et al.*, 1995). This leads to the fundamental question: how far or close should the translational seismometers be placed to obtain a reliable approximation of the rotational field? This is not an easy question to answer because it depends on the properties of the material that is between the seismic stations (see Fig. 1). From a theoretical perspective, the problem remains the same. It means that the conventional theory of elasticity is unable to see local heterogeneities smaller than the grid-size spacing selected in the numerical simulation. This problem has been attempted to be solved using homogenization techniques (Fichtner *et al.*, 2013; Capdeville *et al.*, 2013), but it still remains an approximation of the exact rotational field.

Unlike translational seismology, the development of rotational seismology and rotational sensors (Schreiber *et al.*, 2006; Bernauer *et al.*, 2009; Ferreira and Igel, 2009; Wassermann *et al.*, 2009) provide us direct measures of rotations at single points, or local rotations (Suryanto *et al.*, 2006). This challenges the theory of linear elasticity—as shown previously, linear elasticity cannot measure local rotations, which are instead obtained from finite-difference approximations of the curl operator—and justifies the exploration of alternative theories of wave propagation for including local rotations such as micropolar theory.

Equations of Motion

The equation of motion of micropolar media can be found using the variational formalism of minimum action or Lagrangian approach (Whitham, 1973), which minimizes the action integral I of the form

$$I = \int_0^t \int_\Omega \mathcal{L} d^3\boldsymbol{x} dt = \int_0^t \int_\Omega (K - \mathcal{E}) d^3\boldsymbol{x} dt, \quad (3)$$

in which Ω denotes the volume of the continuum, $\mathcal{L}$ is the Lagrangian defined as the difference between kinetic K and potential energy $\mathcal{E}$. Thus, the Lagrangian approach solves the

minimization problem $\delta I = 0$ to find the governing equations of motion. To find equations of motion including microstructure, we should be able to define the kinetic energy K and potential energy $\mathcal{E}$, also called internal elastic free energy.

The general internal elastic free energy $\mathcal{E}$ for the linear micropolar continuum can be written in index notation as follows:

$$\mathcal{E}(e, \varpi) = \underbrace{\frac{1}{2}e_{ij}\mathbb{C}_{ijkl}e_{kl}}_{\text{elastic free energy}} + \underbrace{\frac{1}{2}\varpi_{ij}\mathbb{H}_{ijkl}\varpi_{kl}}_{\text{rotational elastic free energy}}, \quad (4)$$

in which $e = e_{ij}$ is the second-order strain tensor, $\varpi = \varpi_{ij}$ is the second-order curvature tensor (curvature-twist tensor), and $\mathbb{C} = \mathbb{C}_{ijkl}$ $\mathbb{H} = \mathbb{H}_{ijkl}$ are the fourth-order tensors of elastic constants with the symmetry $\mathbb{C}_{ijkl} = \mathbb{C}_{klij}$ and $\mathbb{H}_{ijkl} = \mathbb{H}_{klij}$, respectively.

The strain e and curvature ϖ tensors have been defined by Eringen (1999) as follows:

$$e_{ij} = \underbrace{\frac{1}{2}\left(\frac{\partial u_i}{\partial x_j} + \frac{\partial u_j}{\partial x_i}\right)}_{\text{symmetric part}} + \underbrace{\epsilon_{ijk}\left(\frac{1}{2}\epsilon_{kab}\frac{\partial u_b}{\partial x_a} - \theta_k\right)}_{\text{antisymmetric part}}, \quad \text{strain tensor}$$

$$\varpi_{ij} = \frac{1}{2}\left(\frac{\partial \theta_i}{\partial x_j} + \frac{\partial \theta_j}{\partial x_i}\right) + \frac{1}{2}\left(\frac{\partial \theta_i}{\partial x_j} - \frac{\partial \theta_j}{\partial x_i}\right), \quad \text{curvature tensor},$$

$$(5)$$

in which the variable u denotes the usual macrodisplacement and θ denotes the spin or microrotation vector. The symbol ϵ refers to the Levi-Civita alternating tensor. The curl operator for vector fields has the well-known expression $(\text{curl}\, u)_k = \epsilon_{kab}u_{b,a}$. In the rest of the article, we will use without distinction the terms "spin" and "microrotation" to denote the field θ.

The main difference between the linear elastic and the linear micropolar models is the presence of the antisymmetric part in the strain tensor e_{ij} (see equation 5). The linear elastic model only contains the symmetric expression. The antisymmetric part in equation (5) is given by the difference between the macrorotation $1/2\,\text{curl}\, u$ and microrotation θ. This means that the linear micropolar model allows the macrorotation to be different from the microrotation; if they are the same, we simply recover the conventional linear elastic model. The assumption of the micropolar model is that this difference adds deformation to the continuum.

To satisfy the conservation of momentum in the Cosserat model, the existence of particle microrotation gives rise to couple stresses, or couples per unit area, in addition to traditional force stresses. The linear micropolar theory thus introduces expressions for the couple-stress relation m in addition to the stress tensor σ as follows:

$$\sigma_{ij} = \frac{\partial \mathcal{E}}{\partial e} = \mathbb{C}_{ijkl}e_{kl}, \qquad m_{ij} = \frac{\partial \mathcal{E}}{\partial \varpi} = \mathbb{H}_{ijkl}\varpi_{kl}, \quad (6)$$

in which σ is the stress tensor and m is the couple-stress tensor or moment-stress tensor (Eringen, 1999).

Considering an isotropic medium and using the definition of the conformally invariant Cosserat model, that is, the couple-stress tensor is invariant under conformal transformations, we can write the linear micropolar stress tensor σ and the couple-stress tensor m as follows:

$$\sigma_{ij} = \underbrace{\mu\left(\frac{\partial u_j}{\partial x_i} + \frac{\partial u_i}{\partial x_j}\right) + \lambda\delta_{ij}\frac{\partial u_k}{\partial x_k}}_{\text{symmetric part}} + \underbrace{2\mu_c\epsilon_{ijk}\left(\frac{1}{2}\epsilon_{kab}\frac{\partial u_b}{\partial x_a} - \theta_k\right)}_{\text{antisymmetric part}},$$

$$m_{ij} = \mu L_c^2\left[\frac{1}{2}\left(\frac{\partial\theta_i}{\partial x_j} + \frac{\partial\theta_j}{\partial x_i}\right) - \frac{1}{3}\frac{\partial\theta_k}{\partial x_k}\delta_{ij}\right] \quad (7)$$

(For further details, see Neff and Jeong, 2009; Neff, Jeong, and Fischle, 2010; Neff, Jeong, Münch, *et al.*, 2010.) The parameters λ, μ [MPa] are the classical Lamé moduli. An elastic constant $\mu_c \geq 0$ [MPa] is introduced, and it is called the "Cosserat couple modulus" because it couples between the macro and the micromedium. If $\mu_c = 0$ in equation (7), we recover the conventional expression for the symmetric stress tensor. The parameter L_c is a characteristic length ($[L_c] =$ meters) of the microstructure related to the problem under study.

Defining the total micropolar kinetic energy as follows:

$$K = \frac{1}{2}\rho\frac{\partial u}{\partial t}\cdot\frac{\partial u}{\partial t} + \frac{1}{2}\eta\cdot\frac{\partial\theta}{\partial t}\cdot\frac{\partial\theta}{\partial t}, \quad (8)$$

in which the center dot represents the dot product, ρ is the macroscopic density and η is the microinertia density tensor of the spin (in the isotropic case, simply a scalar). Solving the minimization problem $\delta I = 0$, with I defined by equation (3), we can find the general linear micropolar equations of motion given by the following expressions:

$$\rho\frac{\partial^2 u}{\partial t^2} = \text{Div}\,\sigma, \qquad \text{balance of linear momentum}$$

$$\eta\frac{\partial^2\theta}{\partial t^2} = \text{Div}\,m + \epsilon : \sigma, \qquad \text{balance of angular momentum},$$

$$(9)$$

in which Div is the divergence of a second-order tensor field defined as $(\text{Div}\,P)_i = \partial P_{ji}/\partial x_j$ and ":" refers to the double scalar product. The free surface boundary conditions are given by

$$\hat{n}\cdot\sigma = \hat{n}\cdot m = 0 \quad \text{on } \partial\Omega, \quad (10)$$

in which $\hat{n}$ refers to the direction normal to the surface $\partial\Omega$.

The equations of motion in linear micropolar media are given by a set of second-order coupled partial differential equations for the displacement-spin fields (see equation 9). A model called the "reduced dynamic Cosserat model"
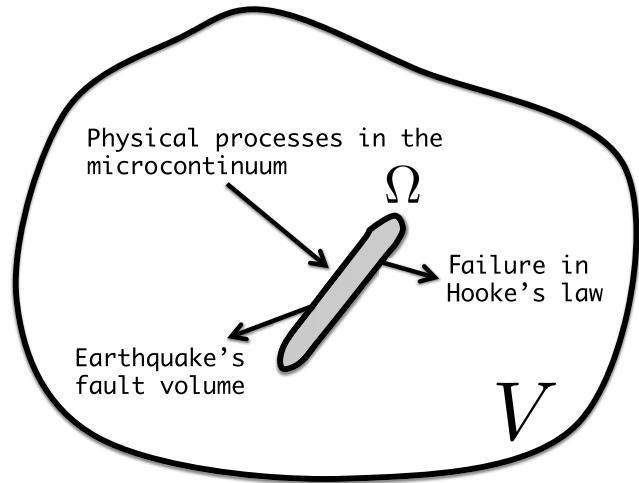
Figure 2. Cartoon representing the failure of Hooke's law within the fault's volume Ω inside the Earth's volume V.

(Grekova *et al.*, 2009; Kulesh *et al.*, 2009; Grekova, 2012a,b, 2016) is obtained considering $L_c = 0$ in equation (7).

Strain and Stress Glut Source

An indigenous source is any phenomenon occurring within or upon the surface of the Earth that does not involve forces exerted by any other bodies. For instance, whereas slip on a fault inside the Earth is an indigenous source, a meteor strike is not. The seismic sources that generate the earthquake's energy are considered indigenous sources (Dahlen and Tromp, 1998).

Because the seismic source energy is generated inside the Earth and no external forces act during the earthquake event, the balance of linear and angular momentum is considered to hold at any moment. The seismic source is then considered to be a localized failure in Hooke's empirical law (equation 7) within a certain region of the space (see Fig. 2). This means that the constitutive relations (equation 7) are valid everywhere except in the earthquake's source region.

The difference between the stress model that satisfies the constitutive Hooke's law and the real (observed or true) stress is called "the stress glut" or "stress excess" (Backus and Mulcahy, 1976a,b; Dahlen and Tromp, 1998). In linear micropolar elastic media, the concept of seismic moment source given by the stress glut can be mathematically defined as follows:

$$\sigma^{\text{glut}} = \sigma^{\text{Hooke}} - \sigma^{\text{true}} \quad \text{and} \quad m^{\text{glut}} = m^{\text{Hooke}} - m^{\text{true}},$$

$$(11)$$

in which σ^{Hooke} and m^{Hooke} refer to the stress and moment stress that satisfy the constitutive Hooke's law in equation (7), and σ^{true} m^{true} refer to the real (observed or true) stress and
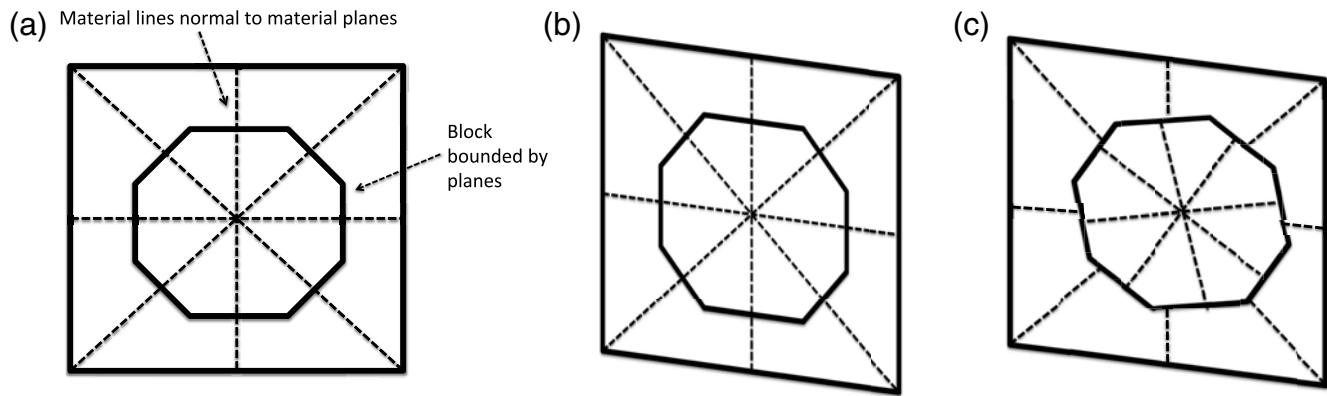
Figure 3. Cartoon representing (a) the undeformed material, (b) the shear deformation in conventional linear elastic, and (c) linear micropolar media. The main difference between the two models is that the linear micropolar model allows internal rigid rotation of the material different from the average continuum rotation $1/2$ curl u assumed in the linear elastic theory (after Twiss *et al.*, 1993).

couple stress that satisfy the equation of motion (the balance of forces in the closed system). The stresses glut in equation (11) are nonzero quantities only within the failure zone.

In a linear micropolar medium, if we substitute the expressions for the stress glut and moment stress glut (equation 11) in the equations of motion (equation 9), we obtain the following:

$$\rho \frac{\partial^2 u}{\partial t^2} = \text{Div}\, \sigma^{\text{Hooke}} - \text{Div}\, \sigma^{\text{glut}}$$

$$\eta \frac{\partial^2 \theta}{\partial t^2} = \text{Div}\, m^{\text{Hooke}} - \text{Div}\, m^{\text{glut}} - \epsilon : \sigma^{\text{Hooke}} + \epsilon : \sigma^{\text{glut}}. \quad (12)$$

Comparing equations (9) and (12), the terms $(-\text{Div}\, \sigma^{\text{glut}})$ and $(\epsilon : \sigma^{\text{glut}} - \text{Div}\, m^{\text{glut}})$ may be understood as equivalent body-force densities for the displacement u and spin θ fields, respectively.

We can now write the linear micropolar equations of motion (equation 12) under the influence of stress glut and moment stress glut, as follows:

$$\rho \frac{\partial^2 u}{\partial t^2} = \text{Div}\, \sigma + f, \qquad \eta \frac{\partial^2 \theta}{\partial t^2} = \text{Div}\, m - \epsilon : \sigma + g, \quad (13)$$

with

$$f = -\text{Div}\, \sigma^{\text{glut}} \quad \text{and} \quad g = -\text{Div}\, m^{\text{glut}} + \epsilon : \sigma^{\text{glut}}. \quad (14)$$

In index notation, we then obtain

$$f_j = -\frac{\partial \sigma_{ij}^{\text{glut}}}{\partial x_i} = -\frac{\partial}{\partial x_i} \mathbb{C}_{ijkl} e_{kl}^{\text{glut}},$$

$$g_j = -\frac{\partial m_{ij}^{\text{glut}}}{\partial x_i} + \epsilon_{jkl} \sigma_{kl}^{\text{glut}} = -\frac{\partial}{\partial x_i} \mathbb{H}_{ijkl} \varpi_{kl}^{\text{glut}} + \epsilon_{jkl} \mathbb{C}_{klmo} e_{mo}^{\text{glut}}.$$
$$(15)$$

Figure 3 shows a shear deformation in conventional linear elastic and linear micropolar media. The undeformed configuration of the medium (Fig. 3a) contains an internal block, which can be understood as a microscopic continuum. In the linear elastic medium, the internal block experiences rigid body rotation in the same material planes of the macroscopic medium (Fig. 3b), but in the linear micropolar medium, it rotates independently of the macroscopic material planes (Fig. 3c).

Green's Tensors

The Green's tensors can be used to represent, in a general way, the solutions of the linear micropolar equations of motion (equation 13) under the influence of the body-force densities (equation 15). The displacement Green's tensor of the medium in the form $G_{qn}(\boldsymbol{r}, t; \boldsymbol{s}, \tau)$ is the qth component of the displacement u_q at the receiver location $\boldsymbol{r}$ and time t, due to an impulsive source of the form

$$f_j(\boldsymbol{r}, t) = \delta_{jn}\delta(\boldsymbol{r} - \boldsymbol{s})\delta(t - \tau), \quad (16)$$

applied in the nth direction at the source location $\boldsymbol{s}$; and time τ (Dahlen and Tromp, 1998; Ampuero and Dahlen, 2005).

In terms of the Green's tensor in classical linear elasticity, we can express the displacement response $u_n(\boldsymbol{r}, t)$ due to an imposed body force $f_j(\boldsymbol{x}, t)$ within a region Ω in the form

$$u_n(\boldsymbol{r}, t) = \int_0^t \int_\Omega G_{nj}(\boldsymbol{r}, t; \boldsymbol{x}, \tau) f_j(\boldsymbol{x}, \tau) d^3\boldsymbol{x} d\tau. \quad (17)$$

In classical linear elasticity, the Green's tensor satisfies the source–receiver reciprocity relationship:

$$G_{qn}(\boldsymbol{r}, t; \boldsymbol{s}, \tau) = G_{nq}(\boldsymbol{s}, t; \boldsymbol{r}, \tau), \quad (18)$$

in which the nth and qth directions must be interchanged, in addition to the locations of the source $\boldsymbol{s}$ and receiver $\boldsymbol{r}$. This means that a source and receiver may be interchanged, and the same waveform will be observed.

In terms of Green's functions in a linear micropolar medium, we can write the displacement $u_n(\boldsymbol{r}, t)$ and spin

$\theta_n(\mathbf{r}, t)$ responses due to impulsive body forces f_j, g_j of the form (equation 16), as follows:

$$\begin{bmatrix} u_n(\mathbf{r},t) \\ \theta_n(\mathbf{r},t) \end{bmatrix} = \int_0^t \int_\Omega \begin{bmatrix} \mathrm{G}_{nj}^{fu}(\mathbf{r},t;\mathbf{x},\tau) \; \mathrm{G}_{nj}^{gu}(\mathbf{r},t;\mathbf{x},\tau) \\ \mathrm{G}_{nj}^{f\theta}(\mathbf{r},t;\mathbf{x},\tau) \; \mathrm{G}_{nj}^{g\theta}(\mathbf{r},t;\mathbf{x},\tau) \end{bmatrix} \begin{bmatrix} f_j(\mathbf{x},\tau) \\ g_j(\mathbf{x},\tau) \end{bmatrix} d^3\mathbf{x}\,d\tau,$$
(19)

in which the Green's tensor G_{nj}^{fu} describes the nth component of the macroscopic displacement $u_n(\mathbf{r}, t)$ at the receiver location $\mathbf{r}$ and time t, due to an impulsive force of the form equation (16) acting on the displacement field. The Green's tensor $\mathrm{G}_{nj}^{g\theta}$ describes the nth component of the microrotation $\theta_n(\mathbf{r}, t)$ at the receiver location $\mathbf{r}$ and time t, due to an impulsive force g_j of the form equation (16) acting in the spin field. The rest of the Green's tensors G^{gu} and $\mathrm{G}^{f\theta}$ can be interpreted in a similar way, that is, the Green's tensor G_{nj}^{gu} describes the nth component of the macroscopic displacement $u_n(\mathbf{r}, t)$ at the receiver location $\mathbf{r}$ and time t, due to an impulsive force of the form equation (16) acting on the spin field and the Green's tensor $\mathrm{G}_{nj}^{f\theta}$ describes the nth component of the microrotation $\theta_n(\mathbf{r}, t)$ at the receiver location $\mathbf{r}$ and time t, due to an impulsive force g_j of the form equation (16) acting in the displacement field.

If we assume that $g = 0$, that is, the only force that generates seismic motion is applied over the displacement field u only, we can write the following solutions:

$$u_n(\mathbf{r}, t) = \int_0^t \int_\Omega \mathrm{G}_{nj}^{fu}(\mathbf{r}, t; \mathbf{x}, \tau) f_j(\mathbf{x}, \tau) d^3\mathbf{x}\,d\tau,$$

$$\theta_n(\mathbf{r}, t) = \int_0^t \int_\Omega \mathrm{G}_{nj}^{f\theta}(\mathbf{r}, t; \mathbf{x}, \tau) f_j(\mathbf{x}, \tau) d^3\mathbf{x}\,d\tau.$$
(20)

On the other hand, if we assume that $f = 0$, the only force that generates seismic motion is applied over the microrotational field θ only, and we can write the following solutions:

$$u_n(\mathbf{r}, t) = \int_0^t \int_\Omega \mathrm{G}_{nj}^{gu}(\mathbf{r}, t; \mathbf{x}, \tau) g_j(\mathbf{x}, \tau) d^3\mathbf{x}\,d\tau,$$

$$\theta_n(\mathbf{r}, t) = \int_0^t \int_\Omega \mathrm{G}_{nj}^{g\theta}(\mathbf{r}, t; \mathbf{x}, \tau) g_j(\mathbf{x}, \tau) d^3\mathbf{x}\,d\tau.$$
(21)

Equations (20) and (21) show that microscales and macroscales are explicitly related with the micropolar description of the seismic source.

Strain and Stress Green's Tensors

The Green's tensors can be used to represent the displacement $u(\mathbf{r}, t)$ and spin $\theta(\mathbf{r}, t)$ responses to a smoothly varying imposed body forces. Inserting equation (15) into equation (19), we can write the following solutions:

$$\begin{bmatrix} u_n(\mathbf{r},t) \\ \theta_n(\mathbf{r},t) \end{bmatrix} = \int_0^t \int_\Omega \begin{bmatrix} \mathrm{G}_{nj}^{fu}(\mathbf{r},t;\mathbf{x},\tau) \; \mathrm{G}_{nj}^{gu}(\mathbf{r},t;\mathbf{x},\tau) \\ \mathrm{G}_{nj}^{f\theta}(\mathbf{r},t;\mathbf{x},\tau) \; \mathrm{G}_{nj}^{g\theta}(\mathbf{r},t;\mathbf{x},\tau) \end{bmatrix}$$
$$\begin{bmatrix} -\frac{\partial}{\partial x_i}\mathbb{C}_{ijkl}e_{kl}^{\mathrm{glut}}(\mathbf{x},\tau) \\ -\frac{\partial}{\partial x_i}\mathbb{H}_{ijkl}\varpi_{kl}^{\mathrm{glut}}(\mathbf{x},\tau)+\epsilon_{jkl}\mathbb{C}_{klmo}e_{mo}^{\mathrm{glut}}(\mathbf{x},\tau) \end{bmatrix} d^3\mathbf{x}\,d\tau.$$
(22)

After integrating by parts and assuming that the boundary term vanishes, we obtain

$$u_n(\mathbf{r}, t) = \int_0^t \int_\Omega \left[\left(\frac{\partial \mathrm{G}_{nj}^{fu}}{\partial x_i} - \epsilon_{ijs}\mathrm{G}_{ns}^{gu} \right) \mathbb{C}_{ijkl}e_{kl}^{\mathrm{glut}} \right.$$
$$\left. + \frac{\partial \mathrm{G}_{nj}^{gu}}{\partial x_i}\mathbb{H}_{ijkl}\varpi_{kl}^{\mathrm{glut}} \right] d^3\mathbf{x}\,d\tau, \theta_n(\mathbf{r}, t)$$
$$= \int_0^t \int_\Omega \left[\left(\frac{\partial \mathrm{G}_{nj}^{f\theta}}{\partial x_i} - \epsilon_{ijs}\mathrm{G}_{ns}^{g\theta} \right) \mathbb{C}_{ijkl}e_{kl}^{\mathrm{glut}} \right.$$
$$\left. + \frac{\partial \mathrm{G}_{nj}^{g\theta}}{\partial x_i}\mathbb{H}_{ijkl}\varpi_{kl}^{\mathrm{glut}} \right] d^3\mathbf{x}\,d\tau.$$
(23)

We define the strain and curvature Green's tensors as follows:

$$E_{nij}^{\boldsymbol{\zeta}}(\mathbf{r}, t; \mathbf{s}, \tau) = \frac{\partial \mathrm{G}_{nj}^{f\boldsymbol{\zeta}}}{\partial \mathbf{r}i} - \varepsilon_{ijs}\mathrm{G}_{ns}^{g\boldsymbol{\zeta}}, \qquad \text{strain Green's tensor}$$

$$C_{nij}^{\boldsymbol{\zeta}}(\mathbf{r}, t; \mathbf{s}, \tau) = \frac{\partial \mathrm{G}_{nj}^{g\boldsymbol{\zeta}}}{\partial \mathbf{r}i}, \qquad \text{curvature Green's tensor} \quad (24)$$

with $\boldsymbol{\zeta} = \{u, \theta\}$.

Unlike in linear elastic media, the strain Green's tensor (equation 24) is not symmetric. This represents a clear advantage of the use of microcontinuum field theories for the description of the seismic source (Twiss, 2009) because the net torque at any point can be represented. (In the Strain and Stress Green's Tensors section, we explain this advantage in more detail.)

We denote the ijth component of stress σ_{ij} and couple-stress tensors m_{ij} at the location $\mathbf{r}$; and time t due to the applied forces f_j, g_j as follows:

$$T_{nkl}^{\boldsymbol{\zeta}}(\mathbf{r}, t; \mathbf{s}, \tau) = \mathbb{C}_{ijkl}(\mathbf{r})E_{nij}^{\boldsymbol{\zeta}}(\mathbf{r}, t; \mathbf{s}, \tau), \text{ stress Green's tensor}$$
$$M_{nkl}^{\boldsymbol{\zeta}}(\mathbf{r}, t; \mathbf{s}, \tau) = \mathbb{H}_{ijkl}(\mathbf{r})C_{nij}^{\boldsymbol{\zeta}}(\mathbf{r}, t; \mathbf{s}, \tau), \text{ couple-stress Green's tensor}$$
(25)

with $\boldsymbol{\zeta} = \{u, \theta\}$. Unlike conventional linear elastic media, the strain, curvature, stress, and couple-stress tensor are no longer symmetric.

We finally write the Green's displacement and spin solutions as follows:
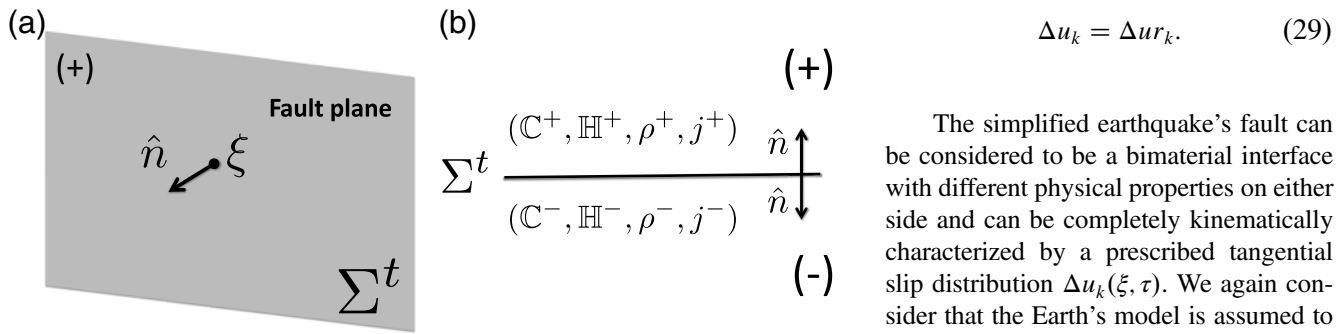
Figure 4.   (a) 2D representation of the seismic fault Σ^t. The superscript t serves as a remainder of the time-dependent nature of the failure process. The symbol $\hat{n}(\xi)$ is the unit normal to the fault at the location ξ. (b) The side toward which the normal points is referred to as the plus $(+)$ or front side of the fault surface, and the opposite side is referred to as the minus $(-)$ or back side.

$$u_n(\boldsymbol{r}, t) = \int_0^t \int_\Omega [E_{ijn}^u \mathbb{C}_{ijkl} e_{kl}^{\text{glut}} + C_{ijn}^u \mathbb{H}_{ijkl} \varpi_{kl}^{\text{glut}}] d^3\boldsymbol{x} d\tau,$$

$$= \int_0^t \int_\Omega [T_{nkl}^u e_{kl}^{\text{glut}} + M_{nkl}^u \varpi_{kl}^{\text{glut}}] d^3\boldsymbol{x} d\tau.$$

$$\theta_n(\boldsymbol{r}, t) = \int_0^t \int_\Omega [E_{ijn}^\theta \mathbb{C}_{ijkl} e_{kl}^{\text{glut}} + C_{ijn}^\theta \mathbb{H}_{ijkl} \varpi_{kl}^{\text{glut}}] d^3\boldsymbol{x} d\tau,$$

$$= \int_0^t \int_\Omega [T_{nkl}^\theta e_{kl}^{\text{glut}} + M_{nkl}^\theta \varpi_{kl}^{\text{glut}}] d^3\boldsymbol{x} d\tau. \qquad (26)$$

Slip on an Ideal Fault

We considered a source specified by a smoothly varying strain glut σ^{glut} and couple-strain glut m^{glut} within a 3D source volume Ω. We now assume that the source region is a plane. Let ξ denote the position of points on the surface Σ^t (the superscript t serves as a remainder of the time-dependent nature of the failure process) and let $\hat{n}(\xi)$ be the unit normal to the fault at ξ. The side toward which the normal points is referred to as the plus $(+)$ or front side of the fault surface, and the opposite side is referred to as the minus $(-)$ or back side (see Fig. 4).

For any function, $w(\xi)$ that is discontinuous across the fault surface Σ^t, we denote

$$w^\pm(\xi) = \lim_{h \to 0} w(\xi \pm h\hat{n}), \qquad (27)$$

the values at juxtaposed points on either side of the fault. In conventional linear elasticity, the tangential slip discontinuity $\Delta u_k(\xi, \tau)$ of the front side relative to the back side is given by the following expression:

$$\Delta u_k = u_k^+ - u_k^-. \qquad (28)$$

The magnitude of the slip vector Δu_k is denoted by $\Delta u(\xi, \tau)$ and its instantaneous direction (slip direction) by $r_k(\xi, \tau)$, so that

$$\Delta u_k = \Delta u r_k. \qquad (29)$$

The simplified earthquake's fault can be considered to be a bimaterial interface with different physical properties on either side and can be completely kinematically characterized by a prescribed tangential slip distribution $\Delta u_k(\xi, \tau)$. We again consider that the Earth's model is assumed to be perfectly elastic everywhere except on the fault's surface Σ^t, that is, where Hooke's law fails.

We consider that the strain glut e^{glut} and curvature glut ϖ^{glut} are singular distributions (see Dahlen and Tromp, 1998, p. 153, for the case of conventional linear elasticity) given explicitly by the following expressions, respectively

$$e^{\text{glut}} = \int_{\Sigma^t} p_{kl}(\xi, \tau) \delta(\boldsymbol{x} - \xi) d^2\xi, \quad \text{with}$$

$$p_{kl}(\xi, \tau) = \Delta u (\hat{n}_k r_l + \hat{n}_l r_k), \qquad (30)$$

in which r denotes the instantaneous direction (slip direction) and $\hat{n}$ the normal vector to the fault's surface. Expression (30) reveals that the strain glut e^{glut} may be expressed as a sum of potency density functions (p_{kl}) at certain locations ξ determined by the Dirac delta function $\delta(\boldsymbol{x} - \xi)$ distributed across the surface of the fault Σ^t. We refer to $p_{kl}(\xi, \tau) = p_{lk}(\xi, \tau)$ as the potency density tensor.

Following Dahlen and Tromp (1998, chap. 5), we can define the moment density tensor as follows:

$$\mathcal{M}_{ij}^\pm = \mathbb{C}_{ijkl}^\pm p_{kl}, \qquad (31)$$

which can be written in isotropic media as follows:

$$\mathcal{M}_{ij}^\pm = \mu^\pm \Delta u (\hat{n}_j r_i + \hat{n}_i r_j). \qquad (32)$$

In linear micropolar elasticity, Twiss *et al.* (1991) and Unruh *et al.* (1996) define the direction of the slip vector as follows:

$$\nu_m = \frac{1}{L}\left[\frac{1}{2}\left(\frac{\partial \dot{u}_k}{\partial x_j} + \frac{\partial \dot{u}_j}{\partial x_k} \right)\hat{n}_k(\delta_{jm} - \hat{n}_j\hat{n}_m) \right. $$
$$\left. + \epsilon_{mkj}\left(\frac{1}{2}\epsilon_{jab}\frac{\partial \dot{u}_b}{\partial x_a} - \dot{\theta}_j \right)\hat{n}_k \right], \qquad (33)$$

in which dot over the variables denotes derivation with respect to time and L is the magnitude of the shear rate vector, that is, the magnitude of the gradient, normal to the shear plane, of the slip velocity (it has units of inverse time). The quantity between braces […] defines the components of the slip velocity vector per unit distance normal to the shear plane (Twiss, 2009). It is assumed that the unit vector

normal to a micromaterial shear plane is parallel to a unit macromaterial vector. Thus, the asymmetric micropolar moment density tensor can be written as follows:

$$\mathfrak{M}_{ij}^{\pm} = \mathbb{C}_{ijkl}^{\pm}\Delta u\hat{n}_k\nu_l. \tag{34}$$

We can write the following expressions for the micropolar moment density tensor in isotropic media:

$$\begin{aligned}
\mathfrak{M}_{ij}^{\pm} &= \mu^{\pm}\Delta u(\hat{n}_j\nu_i + \hat{n}_i\nu_j) + \mu_c^{\pm}\Delta u(\hat{n}_j r_i - \hat{n}_i\nu_j), \\
&= \Delta u\hat{n}_j\nu_i(\mu^{\pm} + \mu_c^{\pm}) + \Delta u\hat{n}_i\nu_j(\mu^{\pm} - \mu_c^{\pm}). \tag{35}
\end{aligned}$$

Assuming that the walls of the fault are not allowed to separate or to interpenetrate, the conditions $\Delta u \cdot \hat{n} = 0$ and $\Delta\theta \cdot \hat{n} = 0$ must be fulfilled, in addition to the condition that the displacement and spin slips must vanish on the instantaneous edge $\partial\Sigma^t$ of the fault, except where that edge may intersect the solid surface of the Earth or the sea floor.

It is noteworthy that the micropolar moment density tensor $\mathfrak{M}_{ij}^{\pm}$ is asymmetric and that the antisymmetric part is governed by the Cosserat couple modulus μ_c. Therefore, in linear micropolar media (equation 35), unlike in linear elastic media (equation 32), the moment density tensor is no longer symmetric. This property of the linear micropolar theory has been noted before (Twiss *et al.*, 1993; Twiss and Unruh, 2007; Twiss, 2009; Twiss and Marrett, 2010). Nonetheless, the contribution in this work is to explicitly relate symmetric and asymmetric parts to elastic constants.

The stress glut σ^{glut} may be written in terms of the moment density tensor as follows:

$$\sigma_{ij}^{\text{glut}} = \int_{\Sigma^t} \mathfrak{M}_{ij}^{\pm}(\xi,\tau)\delta(x-\xi)d^2\xi = \mathfrak{M}_{ij}^{\pm}\delta_{\Sigma'}, \tag{36}$$

in which δ_Σ denotes the Dirac delta function located on the fault surface Σ^t.

Because the moment density tensor is written in terms of the average slip Δu, we can assume $\varpi_{kl}^{\text{glut}} = 0$. Thus, the displacement u and spin θ solutions can be respectively written as follows:

$$\begin{aligned}
u_n(\boldsymbol{r},t) &= \int_0^t \int_{\Sigma^t} E_{ijn}^u(\boldsymbol{r},t;\boldsymbol{\xi},\tau)\mathfrak{M}_{ij}^{\pm}(\boldsymbol{\xi},\tau)d^2\boldsymbol{\xi}d\tau, \\
\theta_n(\boldsymbol{r},t) &= \int_0^t \int_{\Sigma^t} E_{ijn}^\theta(\boldsymbol{r},t;\boldsymbol{\xi},\tau)\mathfrak{M}_{ij}^{\pm}(\boldsymbol{\xi},\tau)d^2\boldsymbol{\xi}d\tau. \tag{37}
\end{aligned}$$

Solutions in equation (37) allow to explicitly relate the displacement and spin responses to the moment density tensor $\mathfrak{M}$, which has been previously studied in kinematic inversions in real field cases (Twiss *et al.*, 1991; Unruh *et al.*, 1996, 2003; Wojtal, 2001; Lewis *et al.*, 2008; Schemmann *et al.*, 2008).

Discussion and Conclusions

We have shown that the use of linear micropolar theory for the description of the earthquake's fault process provides more enriched kinematics of the physics of the earthquake's rupture compared with the classical description. It yields an asymmetric moment tensor that can be used in future studies to fit observed asymmetric fault displacement (see, e.g., Peltzer *et al.*, 1999), and it now depends on a new elastic constant, the Cosserat couple modulus μ_c, that should be included in the future source mechanism inversions. These results are in agreement with previous works that show that the application of micropolar theory has allowed to derive the effects of rigid block rotations on the slip directions (Twiss *et al.*, 1991) and on the asymmetric part of the generalized micropolar seismic moment tensor (Twiss *et al.*, 1993).

The micropolar theory accounts for the existence of an independent rotation or spin θ different from the continuum rotation $1/2\,\text{curl}\,u$. This allows a momentum exchange between the rotational microstructure in the source region and the rest of the Earth. Since the 1960s, many analyses of earthquake source mechanisms have explicitly excluded net forces and torques from consideration (e.g., Julian *et al.*, 1998; Miller *et al.*, 1998; Vavryčuk, 2002; Foulger *et al.*, 2004; Šílený *et al.*, 2009). Because the stress glut in the conventional theory of elasticity is symmetric, there is no net torque at any point (Backus and Mulcahy, 1976b; Dahlen and Tromp, 1998). A more complete analysis including the effects of gravitation and mass advection, however, shows that the conventional linear equation of motion is based on overly restrictive assumptions and that net force and torque components are possible for realistic sources within the Earth (Julian *et al.*, 1998).

Julian *et al.* (1998) show that these kind of forces arise from (1) differences between the Earth's true density distribution and that in Hooke's model, (2) time variations in density caused by mass advection, (3) differences between true particle acceleration and that obtained by linearizing the Eulerian description of motion, (4) differences between the true gravitational acceleration and that in the model, and (5) variations in gravity caused by the mass variations (effects 1 and 2). The unbalanced forces and torques arising from these effects transfer linear and angular momentum between the source region and the rest of the Earth, with both types of momentum conserved for the entire Earth (Julian *et al.*, 1998).

The linear micropolar theory helps describe independent rigid body rotations of internal blocks in brittle deformation processes (Twiss *et al.*, 1993; Twiss, 2009) taking into account the net torque. The focal mechanism plot of a strike-slip fault is shown in Figure 5a. It is impossible to distinguish the case of the right-lateral slip on an east–west-striking fault from left-lateral slip on a north–south-striking fault (e.g., Dahlen and Tromp, 1998; Aki and Richards, 2002). The micropolar focal mechanism plot shown in Figure 5b provides an asymmetric pattern which allows to distinguish the ambiguity inherent to
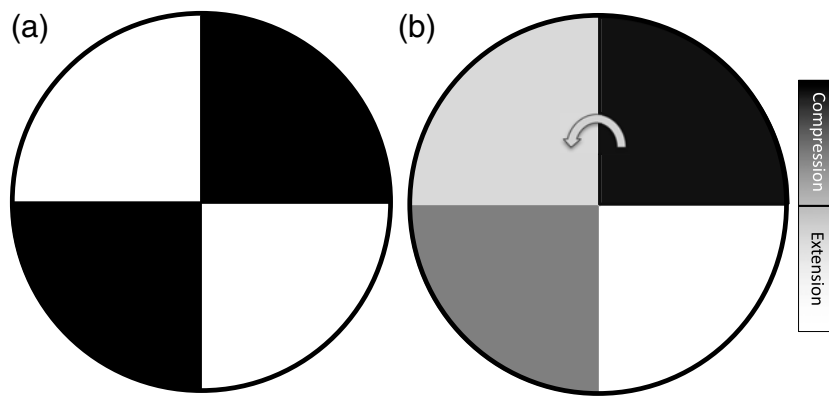
Figure 5. Comparison between the (a) conventional and (b) micropolar focal mechanism plot representations of the moment tensor of a strike-slip fault. The darker color in (b) has been used to represent compression, and the lighter color represent extension, thus allowing rotation.

the traditional representation, clearly showing that the pattern of the fault is north–south-striking.

One possible way forward is to use micropolar theory combined with information provided by rotational seismometers. Rotational seismology is an emerging field and it has recently been proposed that it could provide more information on, for example, rupture processes, anisotropic wave propagation, and normal modes of the Earth among many others applications (Schreiber *et al.*, 2006; Suryanto *et al.*, 2006; Bernauer *et al.*, 2009; Ferreira and Igel, 2009; Lee *et al.*, 2009; Wassermann *et al.*, 2009, 2016; Lee, 2013; Nader *et al.*, 2015; Tanimoto *et al.*, 2015; van Driel *et al.*, 2015; Donner *et al.*, 2016; Reinwald *et al.*, 2016). This work provides a theoretical framework for the development of future dynamic source inversions using micropolar theory on the basis that coseismic block rotations have an observable effect on focal mechanism solutions.

There must be, however, a balance between the complication of mathematical theories of wave propagation and the advantages that these theories may bring to science. Using the micropolar theory, we are introducing more parameters in the wave propagation problem such as the microinertia density η, the characteristic length scale L_c, and the Cosserat couple modulus μ_c. There have been recent attempts to explain the influence of the new parameters in wave propagation and to evaluate them from Earth's mantle materials (Abreu, Kamm, *et al.*, 2017; Abreu, Thomas, *et al.*, 2017) for a more complete picture. With the information provided by the kinematic inversions done using the micropolar model (Twiss *et al.*, 1991; Unruh *et al.*, 1996, 2003; Wojtal, 2001; Lewis *et al.*, 2008; Schemmann *et al.*, 2008), it should be feasible to make micropolar full-waveform source inversions using the adjoint method (Hingee *et al.*, 2011). This then needs to be tested against observations to fully explore the potential of the new theory.

Data and Resources

No data were used in this article.

References

Abreu, R., J. Kamm, and A.-S. Reiß (2017). Micropolar modelling of rotational waves in seismology, *Geophys. J. Int.* **210,** no. 2, 1021.

Abreu, R., C. Thomas, and S. Durand (2017). Effect of observed micropolar motions on wave propagation in deep earth minerals, *Phys. Earth Planet. In.* **276,** 215–225.

Aki, K., and P. G. Richards (2002). *Quantitative Seismology*, Second Ed., University Science Books, Sausalito, California.

Ampuero, J.-P., and F. A. Dahlen (2005). Ambiguity of the moment tensor, *Bull. Seismol. Soc. Am.* **95,** no. 2, 390–400.

Ampuero, J.-P., J.-P. Vilotte, and F. Sanchez-Sesma (2002). Nucleation of rupture under slip dependent friction law: Simple models of fault zone, *J. Geophys. Res.* **107,** no. B12, doi: 10.1029/2001JB000452.

Backus, G., and M. Mulcahy (1976a). Moment tensors and other phenomenological descriptions of seismic sources—I. Continuous displacements, *Geophys. J. Roy. Astron. Soc.* **46,** no. 2, 341–361.

Backus, G., and M. Mulcahy (1976b). Moment tensors and other phenomenological descriptions of seismic sources—II. Discontinuous displacements, *Geophys. J. Roy. Astron. Soc.* **47,** no. 2, 301–329.

Bernauer, M., A. Fichtner, and H. Igel (2009). Inferring earth structure from combined measurements of rotational and translational ground motions, *Geophysics* **74,** no. 6, WCD41–WCD47.

Capdeville, Y., E. Stutzmann, N. Wang, and J.-P. Montagner (2013). Residual homogenization for seismic forward and inverse problems in layered media, *Geophys. J. Int.* **194,** no. 1, 470–487.

Choy, T. (2016). *Effective Medium Theory: Principles and Applications*, Second Ed., Oxford University Press, Oxford, United Kingdom.

Cosserat, E., and F. Cosserat (1909). *Théorie des Corps Déformables*, Librairie Scientifique A. Hermann et Fils, Paris, France (English translation by D. Delphenich 2007, pdf available at https://www.uni-due.de/~hm0014/Cosserat_files/Cosserat09_eng.pdf, last accessed March 2018), reprint 2009 by Hermann Librairie Scientifique, ISBN: 978 27056 6920 1 (in French).

d'Agostino, M. V., G. Barbagallo, I.-D. Ghiba, B. Eidel, P. Neff, and A. Madeo (2018). *Effective Description of Anisotropic Wave Dispersion in Mechanical Band-Gap Metamaterials via the Relaxed Micromorphic Model*, available at https://arxiv.org/abs/1709.07054 (last accessed March 2018).

Dahlen, F., and J. Tromp (1998). *Theoretical Global Seismology*, Princeton University Press, Princeton, New Jersey.

de la Puente, J., J.-P. Ampuero, and M. Käser (2009). Dynamic rupture modeling on unstructured meshes using a discontinuous Galerkin method, *J. Geophys. Res.* **114,** no. B10, doi: 10.1029/2008JB006271.

Donner, S., M. Bernauer, and H. Igel (2016). Inversion for seismic moment tensors combining translational and rotational ground motions, *Geophys. J. Int.* **207,** 562–570.

Eringen, C. (1999). *Microcontinuum Field Theories. I: Foundations and Solids*, Springer, New York, New York.

Eringen, C., and C. Kafadar (1976). *Polar Field Theories, Continuum Physics*, Vol. IV, Academic Press, New York, New York.

Ferreira, A. M. G., and H. Igel (2009). Rotational motions of seismic surface waves in a laterally heterogeneous Earth, *Bull. Seismol. Soc. Am.* **99,** no. 2B, 1429–1436.

Fichtner, A., J. Trampert, P. Cupillard, E. Saygin, T. Taymaz, Y. Capdeville, and A. Villaseñor (2013). Multiscale full waveform inversion, *Geophys. J. Int.* **194,** no. 1, 534–556.

Foulger, G., B. Julian, D. Hill, A. Pitt, P. Malin, and E. Shalev (2004). Non-double-couple microearthquakes at Long Valley caldera, California, provide evidence for hydraulic fracturing, *J. Volcanol. Geoth. Res.* **132,** no. 1, 45–71.

Gade, M., and S. Raghukanth (2016). Seismic response of reduced micropolar elastic half-space, *J. Seismol.* **20,** no. 3, 787–801.

Grekova, E. (2012a). Linear reduced Cosserat medium with spherical tensor of inertia, where rotations are not observed in experiment, *Mech. Solids* **47,** no. 5, 538–543.

Grekova, E. (2012b). Nonlinear isotropic elastic reduced Cosserat continuum as a possible model for geomedium and geomaterials. Spherical prestressed state in the semilinear material, *J. Seismol.* **16,** no. 4, 695–707.

Grekova, E. (2016). Plane waves in the linear elastic reduced Cosserat medium with a finite axially symmetric coupling between volumetric and rotational strains, *Math. Mech. Solids* **21,** no. 1, 73–93.

Grekova, E., M. Kulesh, and G. Herman (2009). Waves in linear elastic media with microrotations, part 2: Isotropic reduced Cosserat model, *Bull. Seismol. Soc. Am.* **99,** no. 2B, 1423–1428.

Hingee, M., H. Tkalčić, A. Fichtner, and M. Sambridge (2011). Seismic moment tensor inversion using a 3-D structural model: Applications for the Australian region, *Geophys. J. Int.* **184,** no. 2, 949–964.

Jeong, J., and P. Neff (2010). Existence, uniqueness and stability in linear Cosserat elasticity for weakest curvature conditions, *Math. Mech. Solids* **15,** no. 1, 78–95.

Julian, B. R., A. D. Miller, and G. Foulger (1998). Non-double-couple earthquakes 1. Theory, *Rev. Geophys.* **36,** no. 4, 525–549.

Kissel, C., and C. Laj (2012). *Paleomagnetic Rotations and Continental Deformation*, Vol. 254, Springer, Dordrecht, The Netherlands.

Kulesh, M., E. Grekova, and I. Shardakov (2009). The problem of surface wave propagation in a reduced Cosserat medium, *Acoust. Phys.* **55,** no. 2, 218–226.

Lee, W. H. K. (2013). *Rotational Seismology*, 877–879.

Lee, W. H. K., H. Igel, and M. D. Trifunac (2009). Recent advances in rotational seismology, *Seismol. Res. Lett.* **80,** no. 3, 479–490.

Lewis, J. C., A. C. Boozer, A. López, and W. Montero (2008). Collision versus sliver transport in the hanging wall at the Middle America subduction zone: Constraints from background seismicity in central Costa Rica, *Geochem. Geophys. Geosys.* **9,** no. 7, Q07S06, doi: 10.1029/2007GC001711.

Luyendyk, B. P., M. J. Kamerling, and R. Terres (1980). Geometric model for Neogene crustal rotations in southern California, *GSA Bull.* **91,** no. 4, 211–217.

Miguel, L. F. F., J. D. Riera, and L. A. Dalguer (2006). Macro constitutive law for rupture dynamics derived from micro constitutive law measured in laboratory, *Geophys. Res. Lett.* **33,** L03302, doi: 10.1029/2005GL024912.

Miller, A. D., G. R. Foulger, and B. R. Julian (1998). Non-double-couple earthquakes 2. Observations, *Rev. Geophys.* **36,** no. 4, 551–568.

Molnar, P., and D. Qidong (1984). Faulting associated with large earthquakes and the average rate of deformation in central and eastern Asia, *J. Geophys. Res.* **89,** no. B7, 6203–6227.

Nader, M., H. Igel, A. Ferreira, D. Al-Attar, J. Wassermann, and K. Schreiber (2015). Normal mode coupling observations with a rotation sensor, *Geophys. J. Int.* **201,** no. 3, 1482–1490.

Nagahama, H., and R. Teisseyre (2000). *Micromorphic Continuum and Fractal Properties of Faults and Earthquakes*, Academic Press, 425–440.

Neff, P., and J. Jeong (2009). A new paradigm: The linear isotropic Cosserat model with conformally invariant curvature energy, *Z. Angew. Math. Mech.* **89,** no. 2, 107–122.

Neff, P., J. Jeong, and A. Fischle (2010). Stable identification of linear isotropic Cosserat parameters: Bounded stiffness in bending and torsion implies conformal invariance of curvature, *Acta Mech.* **211,** nos. 3/4, 237–249.

Neff, P., J. Jeong, I. Münch, and H. Ramézani (2010). Linear Cosserat elasticity, conformal curvature and bounded stiffness, in *Mechanics of Generalized Continua*, G. Maugin and A. Metrikine (Editors), Advances in Mechanics and Mathematics, Vol. 21, Springer, New York, New York, 55–63.

Nowacki, W. (1986). *Theory of Micropolar Elasticity*, Pergamon Press, Warsaw, Poland.

Pelties, C., J. Puente, J.-P. Ampuero, G. B. Brietzke, and M. Käser (2012). Three-dimensional dynamic rupture simulation with a high-order discontinuous Galerkin method on unstructured tetrahedral meshes, *J. Geophys. Res.* **117,** no. B2, doi: 10.1029/2011JB008857.

Peltzer, G., F. Crampé, and G. King (1999). Evidence of nonlinear elasticity of the crust from the M_w 7.6 Manyi (Tibet) earthquake, *Science* **286,** no. 5438, 272–276.

Pluymakers, A., M. Kobchenko, and F. Renard (2017). How microfracture roughness can be used to distinguish between exhumed cracks and in-situ flow paths in shales, *J. Struct. Geol.* **94,** 87–97.

Raziperchikolaee, S., V. Alvarado, and S. Yin (2014a). Effect of fracture roughness on seismic source and fluid transport responses, *Geophys. Res. Lett.* **41,** no. 5, 1530–1536.

Raziperchikolaee, S., V. Alvarado, and S. Yin (2014b). Microscale modeling of fluid flow-geomechanics-seismicity: Relationship between permeability and seismic source response in deformed rock joints, *J. Geophys. Res.* **119,** no. 9, 6958–6975.

Reinwald, M., M. Bernauer, H. Igel, and S. Donner (2016). Improved finite-source inversion through joint measurements of rotational and translational ground motions: A numerical study, *Solid Earth* **7,** no. 5, 1467–1477.

Renard, F., T. Candela, and E. Bouchaud (2013). Constant dimensionality of fault roughness from the scale of micro-fractures to the scale of continents, *Geophys. Res. Lett.* **40,** no. 1, 83–87.

Schemmann, K., J. R. Unruh, and E. M. Moores (2008). Kinematics of Franciscan complex exhumation: New insights from the geology of Mount Diablo, California, *GSA Bull.* **120,** nos. 5/6, 543.

Schijve, J. (1966). Note on couple stresses, *J. Mech. Phys. Solids* **14,** no. 2, 113–120.

Schreiber, U., G. Stedman, H. Igel, and A. Flaws (2006). Ring laser gyroscopes as rotation sensors for seismic wave studies, in *Earthquake Source Asymmetry, Structural Media and Rotation Effects*, R. Teisseyre, E. Majewski, and M. Takeo (Editors), Springer, 377–390.

Sharbati, E., and R. Naghdabadi (2006). Computational aspects of the Cosserat finite element analysis of localization phenomena, *Comput. Mater. Sci.* **38,** no. 2, 303–315.

Šílený, J., D. P. Hill, L. Eisner, and F. H. Cornet (2009). Non-double-couple mechanisms of microearthquakes induced by hydraulic fracturing, *J. Geophys. Res.* **114,** no. B8, doi: 10.1029/2008JB005987.

Spudich, P., L. K. Steck, M. Hellweg, J. Fletcher, and L. M. Baker (1995). Transient stresses at Parkfield, California, produced by the M 7.4 Landers earthquake of June 28, 1992: Observations from the UPSAR dense seismograph array, *J. Geophys. Res.* **100,** no. B1, 675–690.

Suryanto, W., H. Igel, J. Wassermann, A. Cochard, B. Schuberth, D. Vollmer, F. Scherbaum, U. Schreiber, and A. Velikoseltsev (2006). First comparison of array-derived rotational ground motions with direct ring laser measurements, *Bull. Seismol. Soc. Am.* **96,** no. 6, 2059–2071.

Takei, Y., and M. Kumazawa (1994). Why have the single force and torque been excluded from seismic source models? *Geophys. J. Int.* **118,** no. 1, 20.

Tanimoto, T., C. Hadziioannou, H. Igel, J. Wasserman, U. Schreiber, and A. Gebauer (2015). Estimate of Rayleigh-to-Love wave ratio in the secondary microseism by colocated ring laser and seismograph, *Geophys. Res. Lett.* **42,** no. 8, 2650–2655.

Tarasov, B. (2017). Microcracking process as a base of shear rupture mechanism of extreme dynamics, *Proced. Eng.* **191,** 681–688.

Teisseyre, R. (1973). Earthquake processes in a micromorphic continuum, *Pure Appl. Geophys.* **102,** no. 1, 15–28.

Teisseyre, R. (2008). Friction and fracture induced anisotropy: Asymmetric stresses, in *Physics of Asymmetric Continuum: Extreme and Fracture Processes*, R. Teisseyre, H. Nagahama, and E. Majewski (Editors), Springer, 163–169.

Teisseyre, R. (2011). Why rotation seismology: Confrontation between classic and asymmetric theories, *Bull. Seismol. Soc. Am.* **101,** 1683–1691.

Teisseyre, R., M. Gorski, and K. Teisseyre (2008). Fracture processes: spin and twist-shear coincidence, in *Physics of Asymmetric Continuum: Extreme and Fracture Processes*, R. Teisseyre, H. Nagahama, and E. Majewski (Editors), Springer, 111–122.

Teisseyre, R., M. Takeo, and E. Majewski (2006). *Earthquake Source Asymmetry, Structural Media and Rotation Effects*, Springer, The Netherlands.

Twiss, R. J. (2009). An asymmetric micropolar moment tensor derived from a discrete-block model for a rotating granular substructure, *Bull. Seismol. Soc. Am.* **99,** no. 2B, 1103–1131.

Twiss, R. J., and R. Marrett (2010). Determining brittle extension and shear strain using fault-length and displacement systematics: Part I: Theory, *J. Struct. Geol.* **32,** no. 12, 1960–1977.

Twiss, R. J., and J. R. Unruh (2007). Structure, deformation, and strength of the Loma Prieta fault, northern California, USA, as inferred from the 1989–1990 Loma Prieta aftershock sequence, *Geol. Soc. Am. Bull.* **119,** nos. 9/10, 1079–1106.

Twiss, R. J., G. M. Protzman, and S. D. Hurst (1991). Theory of slickenline patterns based on the velocity gradient tensor and microrotation, *Tectonophysics* **186,** no. 3, 215–239.

Twiss, R. J., B. J. Souter, and J. R. Unruh (1993). The effect of block rotations on the global seismic moment tensor and the patterns of seismic P and T axes, *J. Geophys. Res.* **98,** no. B1, 645–674.

Unruh, J., J. Humphrey, and A. Barron (2003). Transtensional model for the Sierra Nevada frontal fault system, eastern California, *Geology* **31,** no. 4, 327.

Unruh, J. R., R. J. Twiss, and E. Hauksson (1996). Seismogenic deformation field in the Mojave block and implications for tectonics of the eastern California shear zone, *J. Geophys. Res.* **101,** no. B4, 8335–8361.

van Driel, M., J. Wassermann, M. F. Nader, B. Schuberth, and H. Igel (2012). Strain rotation coupling and its implications on the measurement of rotational ground motions, *J. Seismol.* **16,** no. 4, 657–668.

van Driel, M., J. Wassermann, C. Pelties, A. Schiemenz, and H. Igel (2015). Tilt effects on moment tensor inversion in the near field of active volcanoes, *Geophys. J. Int.* **202,** no. 3, 1711–1721.

Vavryčuk, V. (2002). Non-double-couple earthquakes of 1997 January in West Bohemia, Czech Republic: Evidence of tensile faulting, *Geophys. J. Int.* **149,** no. 2, 364–373.

Wang, N., J.-P. Montagner, A. Fichtner, and Y. Capdeville (2013). Intrinsic versus extrinsic seismic anisotropy: The radial anisotropy in reference earth models, *Geophys. Res. Lett.* **40,** no. 16, 4284–4288.

Wassermann, J., S. Lehndorfer, H. Igel, and U. Schreiber (2009). Performance test of a commercial rotational motions sensor, *Bull. Seismol. Soc. Am.* **99,** no. 2B, 1449–1456.

Wassermann, J., A. Wietek, C. Hadziioannou, and H. Igel (2016). Toward a single-station approach for microzonation: Using vertical rotation rate to estimate Love-wave dispersion curves and direction finding, *Bull. Seismol. Soc. Am.* **106,** no. 3, 1316–1330.

Wells, R. E., and P. L. Heller (1988). The relative contribution of accretion, shear, and extension to Cenozoic tectonic rotation in the Pacific Northwest, *GSA Bull.* **100,** no. 3, 325–338.

Whitham, G. B. (1973). *Linear and Nonlinear Waves*, John Wiley & Sons, New York, New York.

Wojtal, S. F. (2001). The nature and origin of asymmetric arrays of shear surfaces in fault zones, *Geol. Soc. Lond. Spec. Publ.* **186,** no. 1, 171–193.

Institut für Geophysik
Westfälische Wilhelms-Universität Münster
Corrensstraße 24
D-48149 Münster
Germany
abreusolorzano@gmail.com